# Figure S1

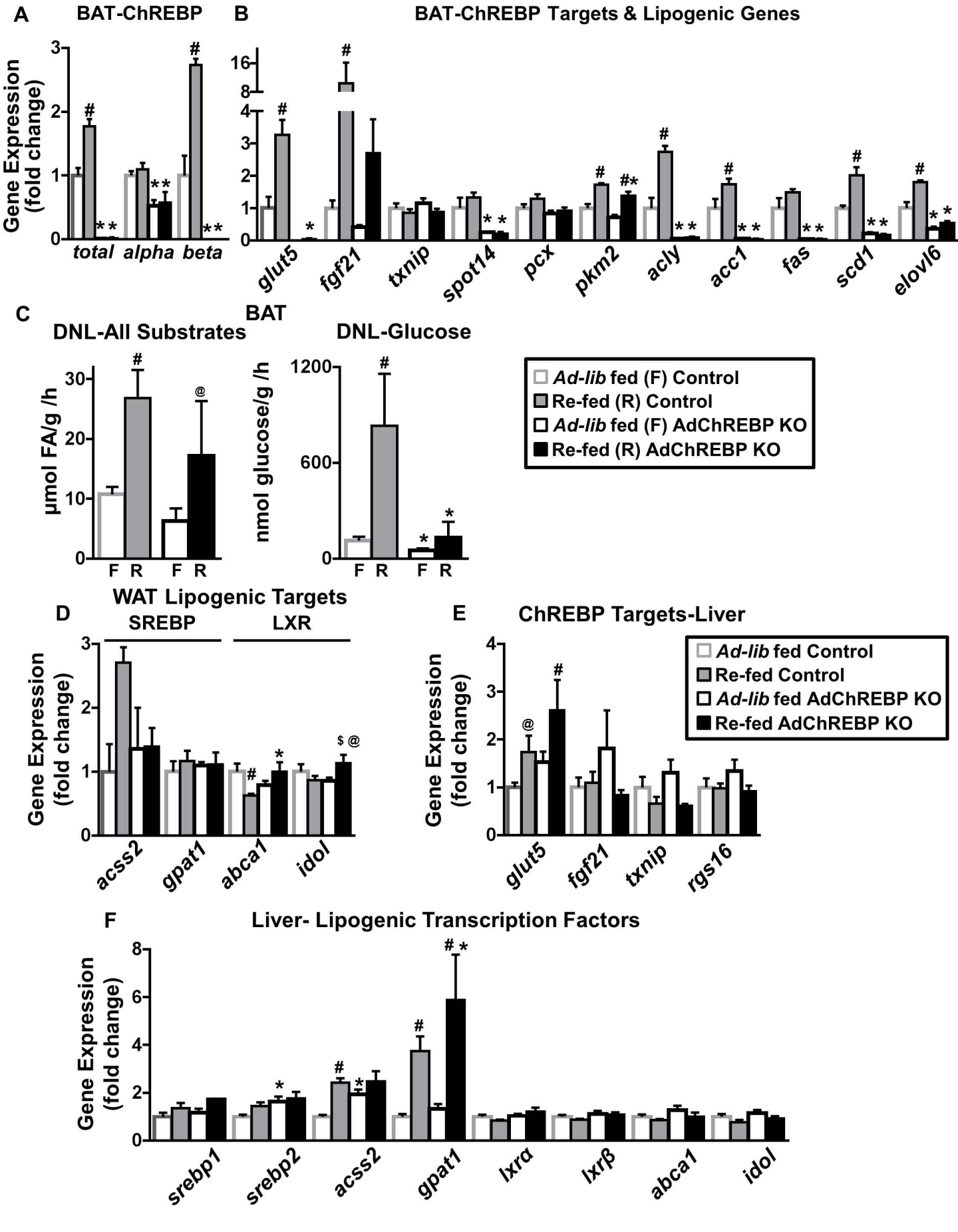
A
BAT-ChREBP
Gene Expression (fold change)
total
alpha
beta
B
BAT-ChREBP Targets & Lipogenic Genes
glut5
fgf21
txnip
spot14
pcx
pkm2
acly
acc1
fas
scd1
elovl6
C
BAT
DNL-All Substrates
µmol FA/g /h
DNL-Glucose
nmol glucose/g /h
F R F R
Ad-lib fed (F) Control
Re-fed (R) Control
Ad-lib fed (F) AdChREBP KO
Re-fed (R) AdChREBP KO
D
WAT Lipogenic Targets
SREBP
LXR
acss2
gpat1
abca1
idol
E
ChREBP Targets-Liver
Ad-lib fed Control
Re-fed Control
Ad-lib fed AdChREBP KO
Re-fed AdChREBP KO
glut5
fgf21
txnip
rgs16
F
Liver- Lipogenic Transcription Factors
srebp1
srebp2
acss2
gpat1
lxrα
lxrβ
abca1
idol

**Supplementary Figure Legends**

**Figure S1. (related to Figure 1) Effect of sucrose re-feeding on DNL in AdChREBP KO mice**

mRNA expression of ChREBP isoforms (A), and ChREBP target and lipogenic enzymes (B), and DNL from all substrates and glucose (C) in BAT of *ad lib*-fed (n=7-11/ genotype) and sucrose re-fed (n=3-5/genotype) female control and AdChREBP KO mice.

(D) mRNA expression SREBP and LXR target genes in PG WAT (n=3-5/genotype/condition).

mRNA expression of ChREBP target genes (E) and lipogenic transcription factors and their target genes (F) in livers of control and AdChREBP KO mice (n=3-5/genotype/condition).

Data are mean ± SEM. mRNA expression was normalized to *tbp* and expressed as fold change over *ad lib*-fed controls. In C, F= *ad lib*-fed and R= sucrose re-fed. *$p< 0.05$; $^{\$}p<0.06$ vs. $ChREBP^{fl/fl}$, same condition; $^{\#}p< 0.05$; $^{@}p<0.06$ vs. *ad lib*-fed, same genotype

# Figure S2

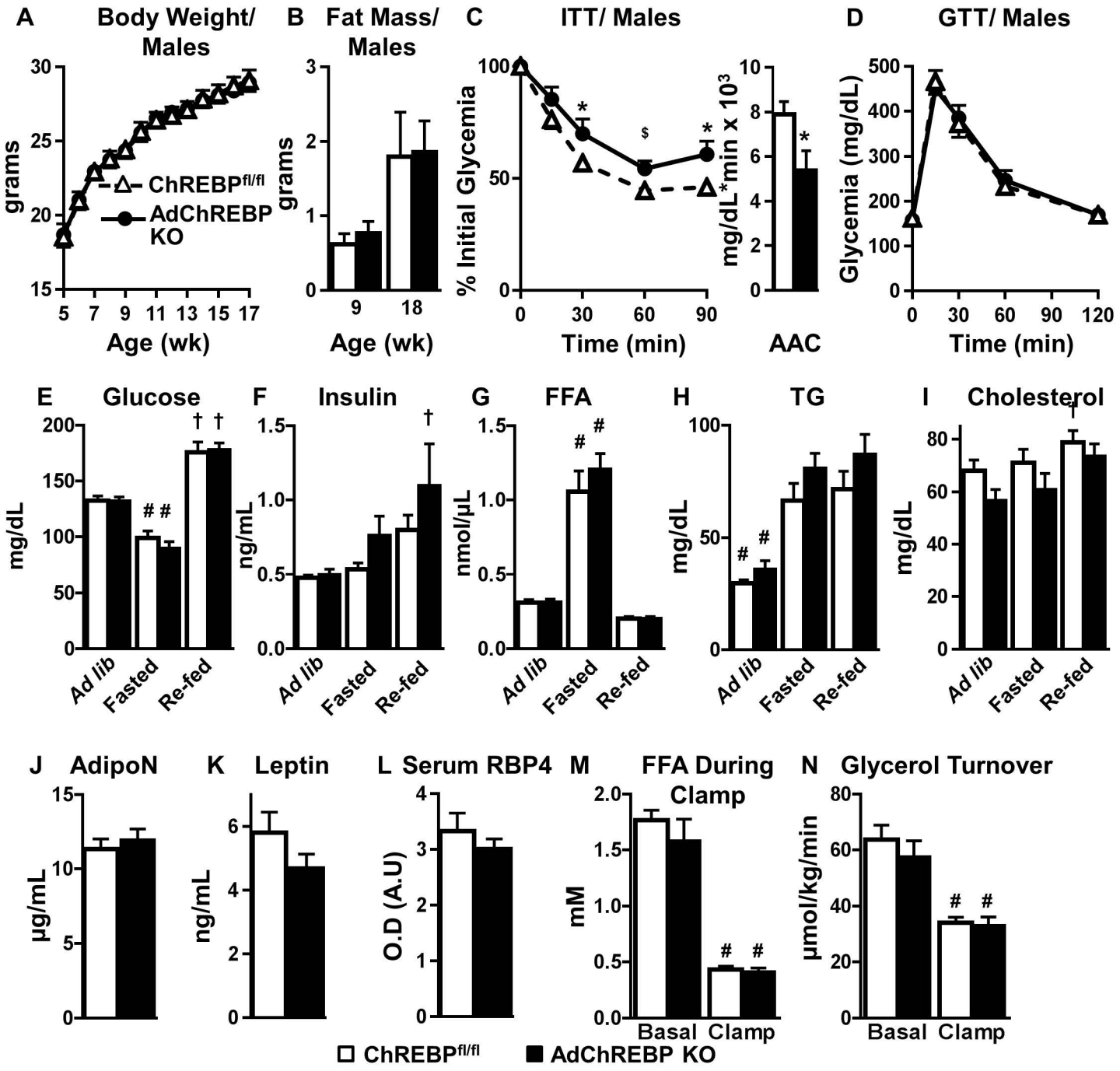


**Figure S2. (related to Figure 2) Phenotype of chow-fed AdChREBP KO mice**

Body weight (A) and fat mass (B) in chow-fed male mice (n=12-14/genotype)

(C) ITT (0.6 U/kg, i.p.) in 6 week-old male mice, 5h after food removal. Data are % fall in glycemia from baseline (n=9-13/genotype).

(D) GTT (2g/kg, i.p.) in 10 week-old male mice by GTT, 8h after food removal (n=7-12/genotype).

Glycemia (E), and serum insulin (F), FFA (G), TG (H) and cholesterol (I) levels in *ad lib*-fed, 12h fasted and 3h re-fed states in female mice (n=13-14/genotype). †-$p<0.05$ vs. *ad lib*-fed, same genotype; #-$p<0.05$ vs. all, same genotype.

Serum adiponectin (AdipoN) (J), leptin (K) and RBP4 (L) in *ad lib*-fed female AdChREBP KO mice (n=13-14/genotype).

Serum FFAs (M) and glycerol turnover (N) in basal and at the end of hyperinsulnemic-euglycemic clamps in overnight fasted chow-fed female mice (n=8/genotype). #$p< 0.05$ vs. basal, same genotype.

**Figure S3**

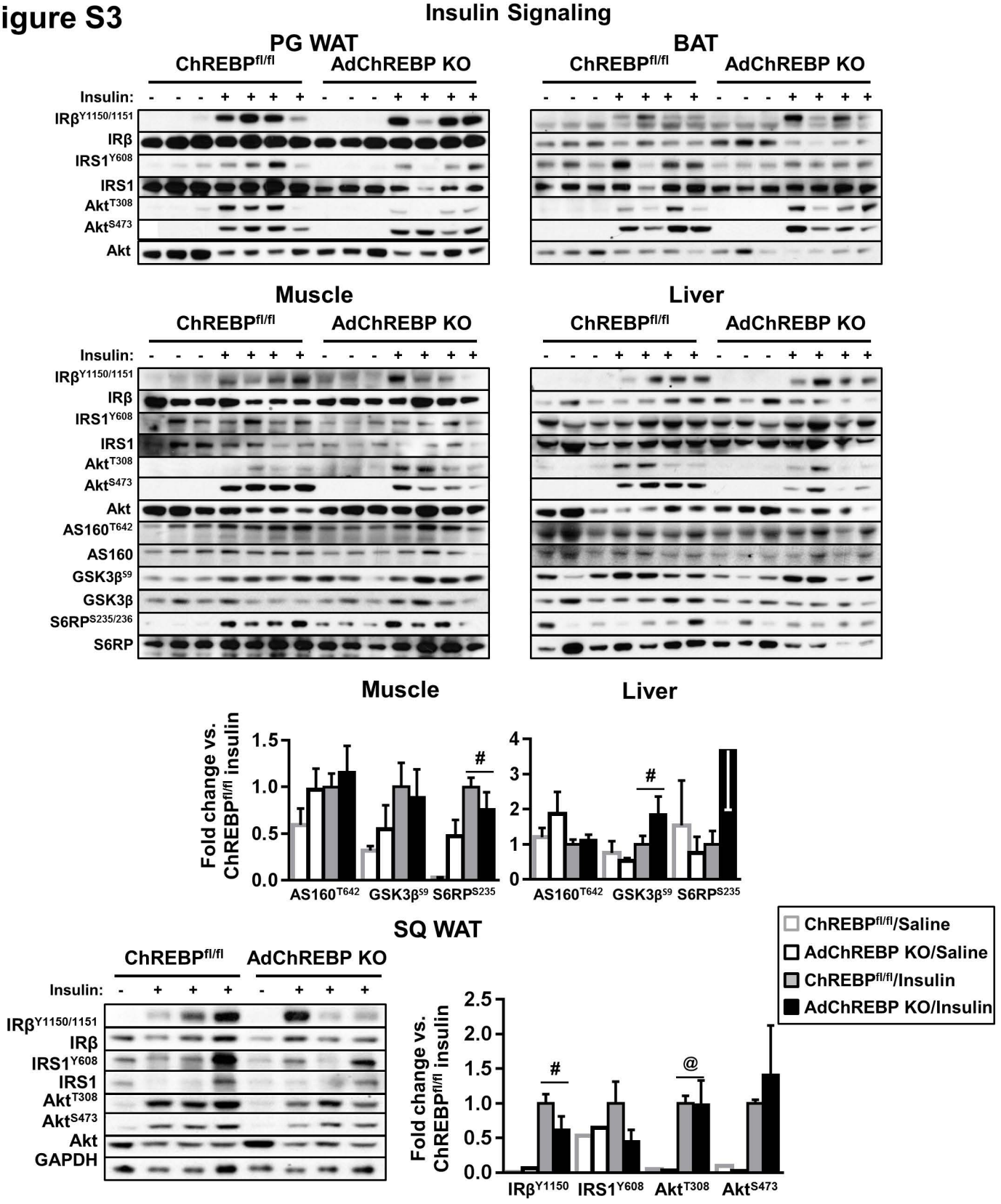


**Figure S3. (related to Figure 2) Insulin signaling in chow-fed AdChREBP KO mice**

Western blotting analysis of insulin signaling intermediates in chow-fed female mice. Levels of phosphorylated proteins were normalized to total levels of respective protein and expressed as a fold change over saline-treated ChREBP$^{fl/fl}$.

Data are mean ± SEM. *p< 0.05 vs. ChREBP$^{fl/fl}$/insulin $^{\#}$p< 0.05 (Two-Way ANOVA), $^{@}$p< 0.05 (t-test) vs. saline.

# Figure S4

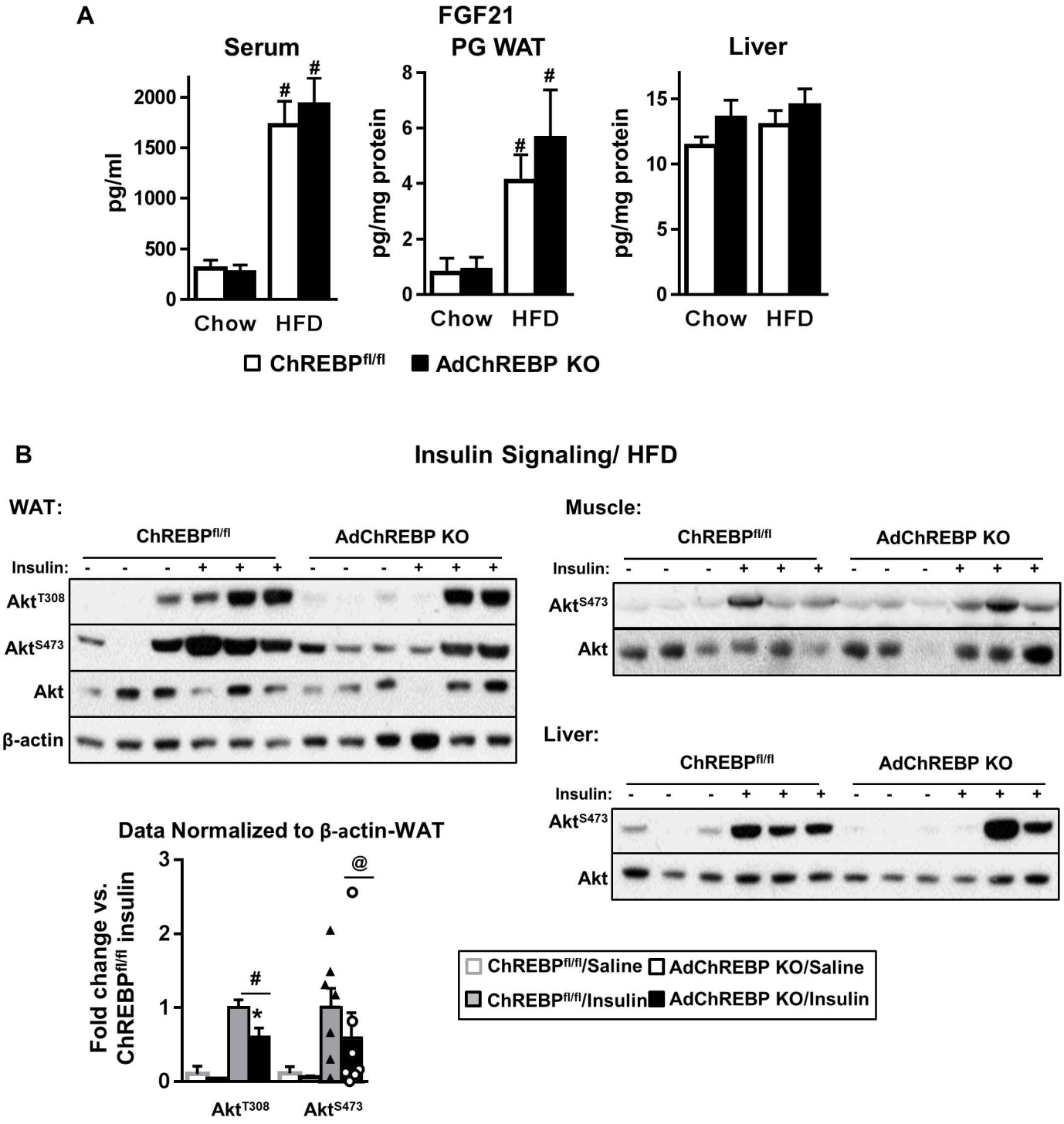


**Figure S4. (related to Figure 4) Effect of HFD feeding in AdChREBP KO mice.**
Serum, PG WAT, and liver FGF21 protein levels in chow and HFD-fed female mice.
(B) Western blot analysis of insulin signaling intermediates in HFD-fed female mice in WAT (left), muscle and liver (right). Due to variability in total Akt signal in WAT, levels of phosphorylated proteins were normalized to a loading control (β-actin) and expressed as a fold change over saline-treated ChREBP$^{fl/fl}$.
(n=3-7/ group)
Data are mean ± SEM. *p< 0.05 vs. ChREBP$^{fl/fl}$; #p< 0.05 vs. chow, same genotype.

# Figure S5

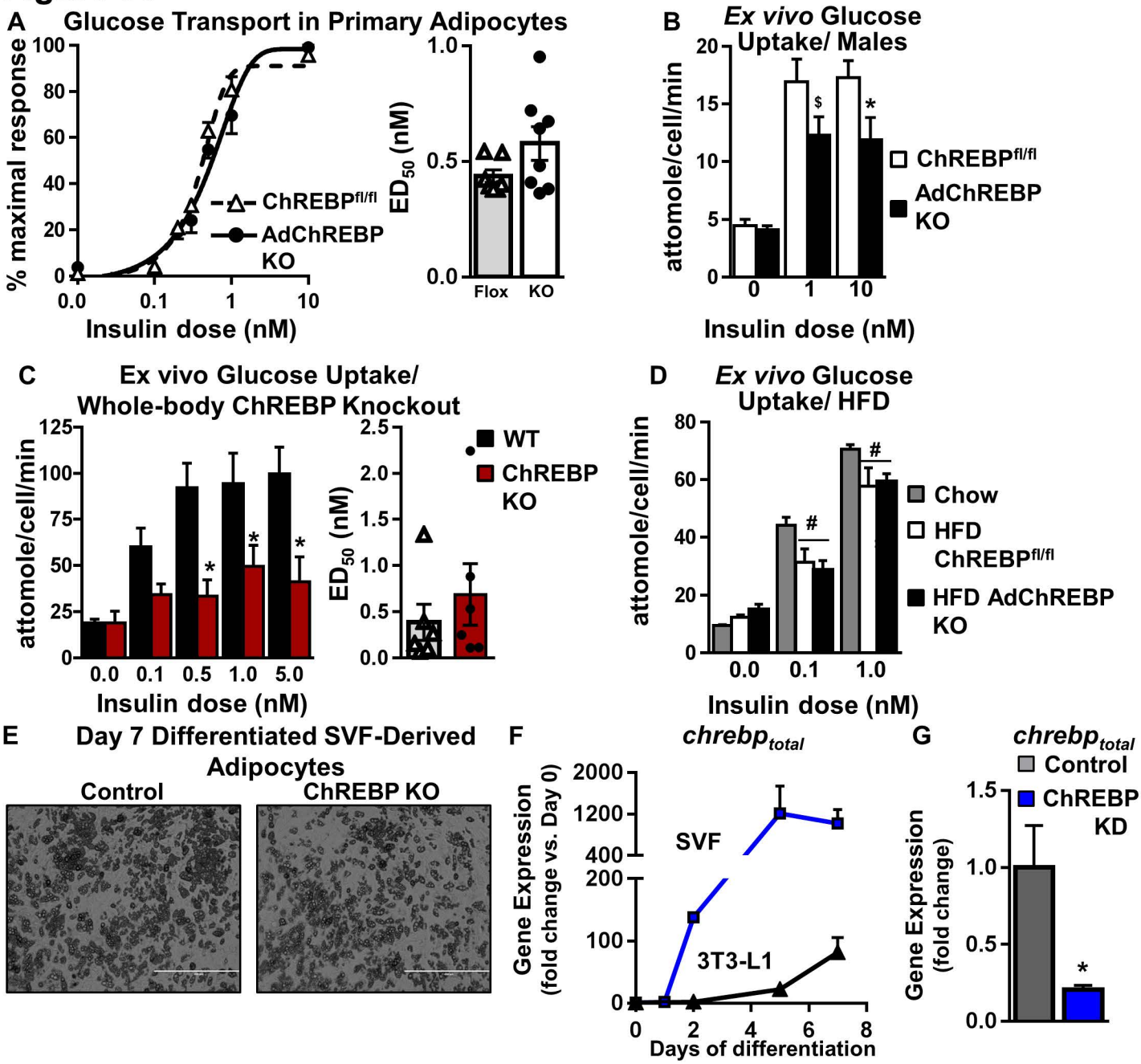


**Figure S5. (related to Figure 5) Adipocytes lacking ChREBP have a cell autonomous reduction in insulin-stimulated glucose transport.**

(A) Insulin-stimulated glucose transport in primary adipocytes isolated from female AdChREBP KO mice expressed as a percentage of maximal glucose uptake (left). Effective dose 50 ($ED_{50}$), or the dose of insulin eliciting half maximal glucose uptake, was calculated for each mouse (right) n= 7-8/genotype.
Insulin-stimulated glucose transport in primary adipocytes isolated from 6 week-old male AdChREBP KO mice (B), 20-24 week-old female whole-body ChREBP KO mice (C), and 8 week HFD-fed female AdChREBP KO mice (D). Data were normalized to adipocyte number. n= 5-9/genotype.
(E) Representative images of Day 7 differentiated SVF-derived adipocytes.
(F) ChREBP mRNA in SVF and 3T3L1 adipocytes over the time course of differentiation. (n=2/group).
(G) ChREBP mRNA expression in 3T3L1 adipocytes treated with scrambled (control) or CHREBP shRNA (ChREBP KD). (n=3-6/group).
Data are mean ± SEM. Gene expression was normalized to *tbp* and expressed as a fold change compared to differentiation Day 0 (E) and control (F). *$p<0.05$, $^{\$}p<0.06$ vs. ChREBP$^{fl/fl}$; $^{\#}p< 0.05$ vs. chow, same genotype.

# Figure S6

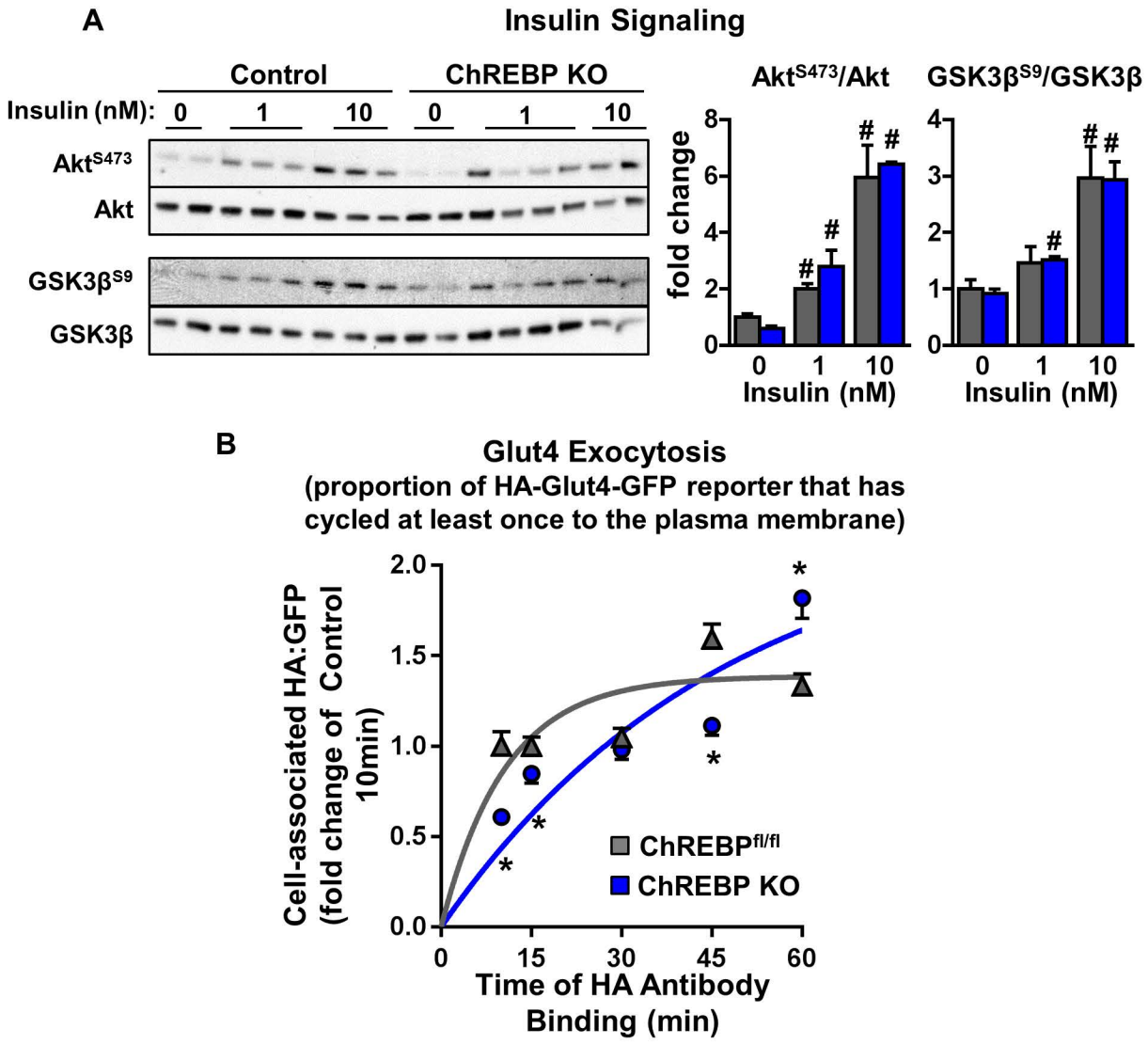


**Figure S6. (related to Figure 6) Loss of ChREBP in adipocytes results in slower insulin-stimulated Glut4 exocytosis.**

(A) Western blot analysis of insulin signaling in control and ChREBP KO adipocytes (left). The ratio of phosphorylated/total protein is expressed as fold change over control basal (0 insulin) (n=2-4/group).

(B) Insulin-stimulated Glut4 exocytosis over a time course in SVF-derived adipocytes. The ratio of cell-associated HA:GFP at any given time point indicates the proportion of the HA-Glut4-GFP reporter that has cycled to the plasma membrane at least once during that time period (Blot and McGraw, 2008). It does not represent the amount of Glut4 at the plasma membrane at any given point of time. The higher value for cell-associated HA:GFP at 60min in the ChREBP KO cells suggests that Glut4 in the pool is still undergoing the first round of exocytosis and therefore, the pool of HA-Glut4-GFP reporter is not completely labelled. Whereas, the entire pool of the HA-Glut4-GFP reporter in the ChREBP$^{fl/fl}$ adipocytes has cycled to the plasma membrane at least once, therefore the signal has reached saturation and the curve has plateaued, so there is no further increase in the ratio for cell-associated HA:GFP. This supports our conclusion of slower Glut4 exocytosis in the ChREBP KO adipocytes. Data are presented as a fold of control at 10min. The data were fit into exponential curve for analysis (n=>100 cells from 2 experiments).

Data are mean±SEM. *$p< 0.05$ vs. control, same condition, # $p< 0.05$ vs. 0 insulin, same genotype.

# Figure S7

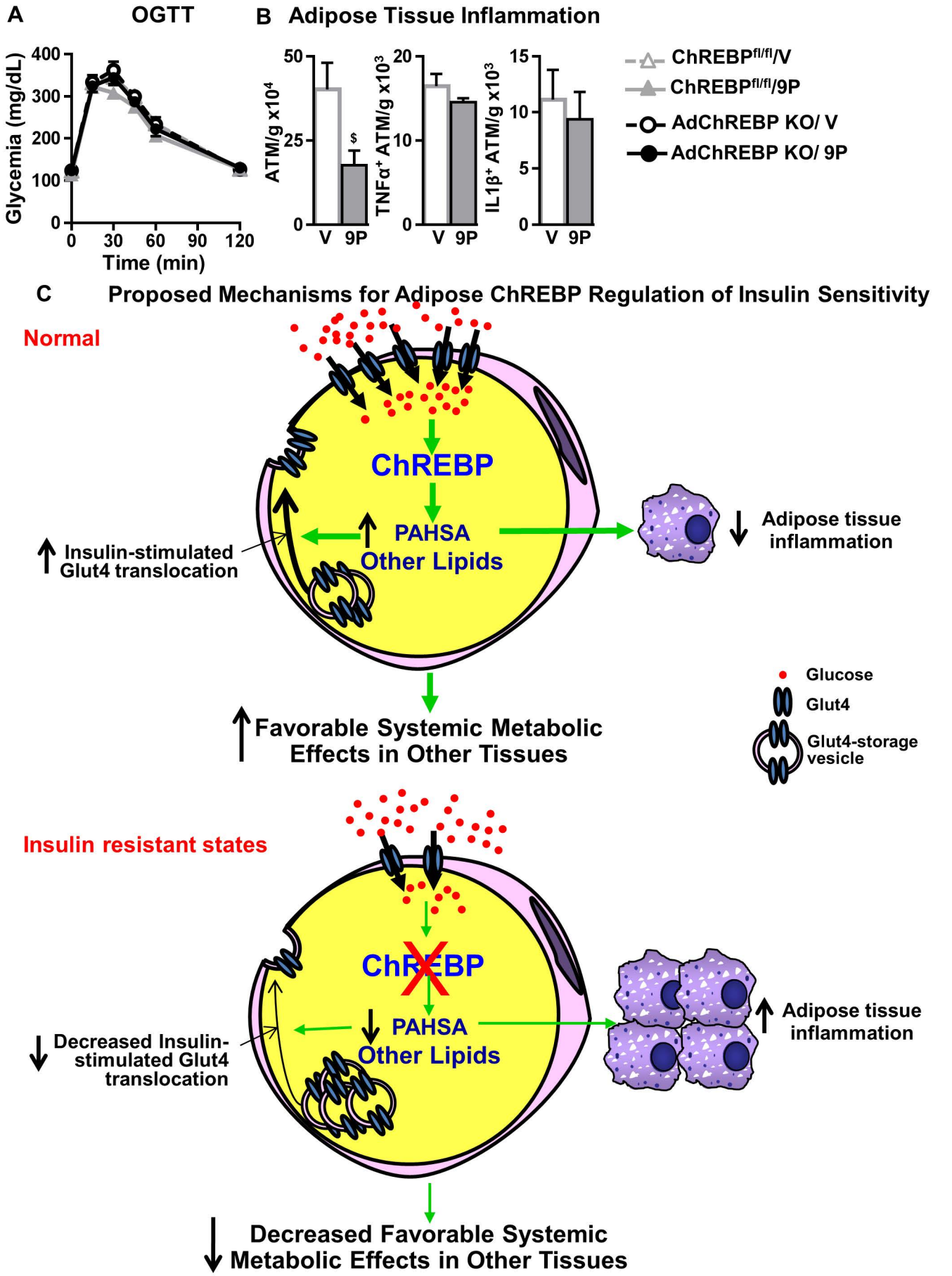
A
OGTT
Glycemia (mg/dL)
400
300
200
100
0
0
30
60
90
120
Time (min)
B
Adipose Tissue Inflammation
ATM/g x10^4
50
25
0
$
V
9P
TNFα+ ATM/g x10^3
20
10
0
V
9P
IL1β+ ATM/g x10^3
15
10
5
0
V
9P
ChREBPfl/fl/V
ChREBPfl/fl/9P
AdChREBP KO/ V
AdChREBP KO/ 9P
C
Proposed Mechanisms for Adipose ChREBP Regulation of Insulin Sensitivity
Normal
ChREBP
PAHSA
Other Lipids
Insulin-stimulated Glut4 translocation
Adipose tissue inflammation
Favorable Systemic Metabolic Effects in Other Tissues
Glucose
Glut4
Glut4-storage vesicle
Insulin resistant states
ChREBP
PAHSA
Other Lipids
Decreased Insulin-stimulated Glut4 translocation
Adipose tissue inflammation
Decreased Favorable Systemic Metabolic Effects in Other Tissues

**Figure S7. (related to Figure 7) Effects of PAHSAs on insulin resistance in absence of adipose-ChREBP.**

(A) GTT (1.5g/kg, oral gavage), in mice treated with vehicle (V) or 9-PAHSA (9P, 15mg/kg/d, oral gavage) for 16 days. n=7-10/ group.

(B) Numbers of total, TNF$\alpha^{+}$ and IL-1$\beta^{+}$ ATMs in PG WAT of ChREBP$^{fl/fl}$ mice treated with vehicle (V) or 9-PAHSA (9P, 15mg/kg/d, oral gavage) for 26 days (n=5/group).

(C) The mechanisms by which altering adipose-ChREBP regulates insulin sensitivity include alterations in PAHSAs and other potentially lipids. In the insulin sensitive (normal) state, glucose flux into adipocytes via Glut4 induces ChREBP and results in higher net synthesis of signaling lipids such as PAHSAs which have multiple biological effects. ChREBP promotes insulin-stimulated adipocyte Glut4 translocation most likely via PAHSA-dependent and/or independent mechanisms, further augmenting insulin-stimulated glucose uptake into adipocytes. ChREBP activity in adipocytes also has favorable effects on adipose tissue inflammation which is most likely mediated by PAHSAs. Adipose-ChREBP also improves insulin sensitivity in other metabolic tissues such as liver and muscle which may be mediated by PAHSAs. Together, these biological effects of adipose-ChREBP promote systemic insulin sensitivity. These beneficial effects of adipose-ChREBP are lost in insulin resistance.

## Extended Experimental Procedures

### Animal studies and measurement of metabolic parameters

All experimental procedures were in accordance with the Institutional Animal Care and Use Committee of Beth Israel Deaconess Medical Center (BIDMC). ChREBP$^{fl/fl}$ mice, a gift from Dr. Jay D. Horton (U.T Southwestern Medical Center), were re-derived into the C57BL/6J background in the Animal Research Facility at BIDMC and were subsequently crossed to Adiponectin-Cre mice (also on the C57Bl/6J background) (Eguchi et al., 2011) to generate AdChREBP KO mice. For our initial studies we crossed ChREBP$^{+/fl}$/Adiponectin-Cre$^{+/-}$ male with ChREBP$^{+/fl}$ female mice to generate the following genotypes; ChREBP$^{+/+}$ (wild-type), Adiponectin-Cre$^{+/-}$, ChREBP$^{fl/fl}$ and ChREBP$^{fl/fl}$/Adiponectin-Cre$^{+/-}$ (AdChREBP KO). We phenotyped all control lines (WT, Adiponectin-Cre$^{+/-}$, and ChREBP$^{fl/fl}$) and saw no differences between the control genotypes with respect to body weight, adiposity, and glucose or insulin tolerance. Therefore, subsequently we switched to breeding AdChREBP KO males with ChREBP$^{fl/fl}$ females, and used ChREBP$^{fl/fl}$ littermates as controls. All mice were on the C57BL/6J background and all studies were performed in age- and sex- matched littermates. The mice had *ad libitum* access to water and either standard mouse chow (LabDiet), or, where indicated, high-fat (55% fat) diet (Harlan Laboratories). Body weight was monitored weekly from 3 weeks of age. Body composition analysis was performed at indicated times using the EchoMRI 3-in-1 NMR system (Echo Medical Systems). Commercially available kits were used for serum measurements of circulating factors such as insulin and leptin (Crystal Chem), adiponectin (RnD Systems), FFA (Wako Chemicals), cholesterol and TG (Pointe Scientific), and FGF21 (Millipore). 2µL of serum was used to determine serum RBP4 levels by western blot analysis as described previously (Moraes-Vieira et al., 2014). Insulin (ITT) and glucose (GTT) tolerance tests were performed in awake mice after 5h food removal or overnight fast, and glycemia was determined using a One Touch Basic glucometer (Lifescan).

### *In vivo* lipogenesis

Rates of lipogenesis are typically low in WAT of *ad lib*-fed mice, unlike the liver which has ~27 fold higher lipogenic rates. Rates of lipogenesis may also be affected by time of last feed (Bruss et al., 2010), and mice eat sporadically throughout most of the day (Ellacott et al., 2010) which introduces significant variability when measuring the relatively low rates of DNL in WAT. Therefore, the sucrose refeeding (Engelking et al., 2004) protocol was employed to synchronize feeding in all mice, and to induce ChREBP and DNL in WAT so that it was more easily detectable. For this, mice were fasted for 12h and re-fed with chow and also received 15% sucrose in drinking water for an additional 12h. *Ad lib*-fed and sucrose re-fed mice received a bolus (i.p.) of 5mCi of [$^{3}$H]-$H_2O$ (American Radiolabeled Chemicals) and 10µCi of [U-$^{14}$C]-glucose (Perkin Elmer), and were sacrificed 1h later for tissue collection. Plasma samples were collected at 5, 10, 30 and 60 minutes for specific activity measurements. Fatty acids were extracted from tissue samples and rates of incorporation of $^{3}$H and $^{14}$C tracers were calculated as described (Herman et al., 2012).

### Hyperinsulinemic-euglycemic clamps

Hyperinsulinemic-euglycemic clamps were performed in awake, overnight fasted 16-20 week-old chow-fed female ChREBP$^{fl/fl}$ and AdChREBP KO mice as per published protocols. 2-deoxyglucose uptake into individual tissues and glycerol turnover were also measured at the end of the clamp as published (Perry et al., 2015; Jurczak et al., 2012).

**9-PAHSA treatment studies**
7-9 week-old male mice were treated chronically for once a day with vehicle (50% PEG-400 /0.5% Tween-80/ 49.5% saline) or 15mg/kg of 9-PAHSA by oral gavage between 6:30-7:30pm for 26 days. The dose of PEG400 that we used and even higher has no reported toxicity *in vivo* (2012). All in vivo studies were performed ~12-16h after last 9-PAHSA gavage.

***Ex vivo* glucose uptake in isolated primary adipocytes**
Insulin-stimulated glucose uptake was measured in primary adipocytes isolated from PG WAT as previously described (Carvalho et al., 2004). Briefly, fat pads were digested with 1 mg/ml collagenase (Worthington) and adipocytes were incubated at 37 °C with constant shaking in Krebs-Ringer-HEPES buffer (20mM HEPES pH 7.4, 120mM NaCl, 1.2mM $CaCl_2$, 4.8mM KCl, 0.6mM $MgSO_4$, 1.2mM $KH_2PO_4$) with 2.5% bovine serum albumin and 100nM adenosine in the presence of varying concentrations of insulin (Eli Lily). 30min after insulin stimulation, 3μCi [U-$^{14}$C]-glucose (Perkin Elmer) was added for 30 min and the reaction was terminated by separating cells from incubation buffer by spinning the suspension through dinonyl phthalate oil (Arco Organics). An aliquot of isolated adipocytes from each sample was fixed with osmic acid for cell number determination.

**Adipocyte morphometry**
Adipocyte cell number and cell size were determined in a small, minced piece of WAT of known weight or primary adipocytes as previously published (Herman et al., 2012). Briefly, osmium-fixed samples were filtered through a nylon filter with saline (0.9% sodium chloride) to separate adipocytes from tissue debris. Cell size and number were determined using a Beckman Coulter Multisizer III counter. The cell number and cell size for each sample represents an average of 6 times measurements. Cell number was normalized to tissue weight.

***Ex vivo* lipolysis in adipose tissue explants**
PG WAT was harvested from female mice 6h after food removal, minced into 10-20mg pieces and incubated in Krebs-Ringer-HEPES buffer (20mM HEPES pH 7.4, 120mM NaCl, 1.2mM $CaCl_2$, 4.8mM KCl, 0.6mM $MgSO_4$, 1.2mM $KH_2PO_4$) with 3% bovine serum albumin, 100nM adenosine and 5mM glucose with/without 1mM 8-bromo cAMP (Sigma) and increasing concentrations of insulin. Media was collected after 3.5h and glycerol levels in media were colorimetric determined using manufacturer's instructions (Sigma). Glycerol levels were normalized to tissue weight.

**Flow cytometry**
Isolation of stromal vascular fraction of PG WAT, and staining with antibody for surface markers and intracellular cytokines were performed as previously published (Moraes-Vieira et al., 2014). The cells were acquired on a specially ordered five-laser LSR II flow cytometer (BD Biosciences) are the Flow Cytometry Core facility at BIDMC and analyzed with FlowJo 9.5.3 software (Treestar).

**Insulin signaling**

For *in vivo* insulin signaling studies, mice were injected with an insulin bolus (2U/kg; i.p) 2h after food removal. Mice were sacrificed after 5 min (chow study) or 15 min (HFD study), tissues were harvested and frozen in liquid nitrogen for future analysis.
For *in vitro* insulin signaling studies, SVF adipocytes were serum starved for 3h and incubated with insulin at indicated concentrations for 10min, rinsed with ice-col PBS and frozen until further processing.

**Cell Culture**
Pre-adipocytes from the stromal-vascular fraction (SVF) of the SQ WAT were isolated from 5-8 week old mice as described previously (Aune et al., 2013; Vazirani et al., 2016). Briefly, both fat pads were digested in 5mg/mL Collagenase D (Roche), 2U/mL dispaseII (Roche) and 10mM $CaCl_2$, the SVF cells were separated from adipocytes using 40µm cell strainers and plated overnight in DMEM supplemented with 15% FBS and 1% antibiotic. Unattached cells were subsequently removed with PBS washing. The SVF preadipocytes were maintained in DMEM/15% FBS/1% antibiotic at 37°C and 5%$CO_2$ until confluency. 3T3L1 adipocytes were cultured using standard protocols (Yore et al., 2014). Differentiation was initiated using DMEM containing 10% FBS, 4mg/ml bovine insulin, 0.25mM dexamethasone, 0.5mM 3-isobutyl-1-methylxanthine and 2mM rosiglitazone. On day 2 (for SVFs) and 3 (for 3T3L1s) of differentiation, the media was replaced with DMEM/10% FBS/1% antibiotic. Media was changed every 2 days until cells were used for experimental studies at 7–10 days post-differentiation. ChREBP shRNA lentiviral plasmid (Sigma) was packaged into lentiviral particles in 293T cells using the Lenti-X Packaging system (Clonetech) using manufacturer's instructions. Day 7 and later differentiated 3T3L1 adipocytes were treated with scrambled or ChREBP shRNA for 3-4 days before any experiments.

***In vitro g*lucose uptake in differentiated adipocytes**
*In vitro* glucose uptake assays were performed after 2–3h serum starvation, 30 min glucose starvation in Krebs-Ringer-HEPES (KRH) buffer (50mM HEPES pH 7.4, 136mM NaCl, 1.25mM $CaCl_2$, 4.7mM KCl, 1.25mM $MgSO_4$) and 25 min insulin stimulation. The cells were incubated with 100mM 2-deoxyglucose containing 1µCi of $^3$H-2-deoxyglucose (Perkin Elmer) for 5 min, washed 3 times in ice-cold PBS, solubilized with 1% Triton X-100 to count incorporation of radioactivity in cells which was normalized to protein concentration (Yore et al., 2014).

**Glut4 translocation and exocytosis**
All experiments were performed using published protocols (Blot and McGraw, 2008). All experiments were performed 12-16h after electroporating differentiated SVF adipocytes with HA-GLUT4-GFP plasmid. In all experiments, adipocytes were pre-incubated in serum-free DMEM media for at least 120 min at 37°C in 5% CO2/air (basal conditions). For insulin stimulation, cells were incubated in serum-free DMEM media containing 1nM insulin (Sigma-Aldrich) for 30 min at 37°C in 5% CO2. Cells were washed twice in ice-cold PBS containing $Ca^{2+}$/$Mg^{2+}$ and fixed in 3.7% formaldehyde (Sigma). To measure GLUT4 translocation, cells expressing HA-GLUT4-GFP reporter were stained for surface HA.11 in non-permeabilized cells using indirect immunofluorescence with Cy3-labeled goat anti-mouse IgG, whereas GFP fluorescence is a measure of total HA-GLUT4-GFP per cell. For the exocytosis study, half-time for insulin-stimulated Glut4 exocytosis (t1/2) studied using the HA-Glut4-GFP reporter has been

empirically determined to be between 10-20min after insulin stimulation (Blot and McGraw, 2008; Karylowski et al., 2004). After insulin stimulation, cells were incubated with anti-HA.11 antibody for the indicated times. Cells were fixed, permeablized and stained for HA.11 using indirect immunofluorescence with Cy3-labeled goat anti-mouse IgG and normalized to GFP fluorescence. For 9-PAHSA study, cells were pre-incubated with 9-PAHSA (20μM) for 2h during serum starvation.

**Western blotting**

Proteins were extracted from cells and tissues using protein lysis buffer (50mMTris, 150mM sodium chloride, 1mM EDTA, 10% NP-40, and commercially available protease and phosphatase inhibitor cocktails (Roche)). Post-nuclear membranes were isolated from 250-300 mg PG WAT homogenized in HES buffer (10mM HEPES, 250mM sucrose, 5mM EDTA), centrifuged at 3000rpm for 10min to remove debris and ultra-centrifuged at 100,000rpm for 1h. The resulting post-nuclear membranes were re-suspended in protein lysis buffer. Protein concentrations were determined using the BCA assay, and 25-30μg protein was used for western blotting. Membranes were probed with antibodies against GLUT4 (provided by H. Haspel), phospho insulin receptor (IR)$^{Y1150/1151}$, phosphoAkt$^{S473}$, phosphoAkt$^{T308}$, AKT, phospho glycogen synthase kinase 3 β (GSK3β)$^{S9}$, GSK3β, phospho Akt Substrate 160(AS160)$^{T642}$, phospho S6 ribosomal protein (S6RP)$^{S235/236}$, S6RP (Cell Signaling), phospho insulin receptor substrate 1 (IRS1)$^{Y608}$, IRS1 (Millipore), IR, β-actin, GAPDH (Santa Cruz), and AS160 and PI3K p85 (Millipore). Film images were scanned (Epson Expression 10000 XL) and results were quantified with ImageJ software (NIH).

**Gene Expression**

mRNA was extracted using Trizol reagent (Invitrogen) and RNeasy Mini kit (Qiagen) and reverse transcribed using the Advantage RT for PCR kit (Clontech) using manufacturer's instructions. Quantitative PCR was performed using SYBR Green PCR Master Mix (Applied Biosystems) in a 7900 HT thermocycler (Applied Biosystems). SDS 2.3 (Applied Biosystems) was used for calculation of cycle thresholds. Relative expression levels were determined using the $\Delta\Delta C_t$ method with normalization of target gene expression levels to TATA box binding protein (*tbp*) (Herman et al., 2012).

**Hepatic TG measurements**

Lipids were extracted from 80-100mg of liver by the Folch method using chloroform/methanol/ sodium chloride (2:1:1), the organic phase was dried under a steady stream of nitrogen gas, saponified in 3M potassium hydroxide/ 65% ethanol at 70°C for 1h and TG content were determined using a commercial kit (Pointe Scientific).

**Lipidomic analysis**

Lipids were extracted from 80-100mg WAT tissue, or 80-100μL serum using known protocols (Bligh and Dyer, 1959; Yore et al., 2014; Zhang et al., 2016). Briefly, tissues were Dounce homogenized on ice for 40 strokes in a mixture of 1: 1: 2 citric acid buffer (100mM trisodium citrate, 1M NaCl, pH 3.6): methanol: chloroform. Serum lipids were extracted in 1:1:2 citric acid buffer: methanol: chloroform, shaken for 30s by hand and vortexed for 15s. $^{13}$C-9-PAHSA standard (0.5–5pmol per sample) was added to chloroform prior to extraction. The resulting homogenate was centrifuged at 2,200g, 6 min, 4°C to separate organic and aqueous phases, and

the organic phase containing extracted lipids was removed, dried under a gentle stream of Nitrogen and stored at 80°C. For PAHSA analysis, tissues and serum were subjected to solid phase extraction (SPE) at room temperature via gravity flow. SPE cartridge (500 mg silica, 6ml, Thermo Scientific, 60108-411) was conditioned with 15ml hexane. Extracted lipids (reconstituted in 200µl chloroform) were loaded onto column. Neutral lipids were eluted with 16ml 5% ethyl acetate in hexane, followed by elution of PAHSAs with 16ml ethyl acetate. PAHSA fraction was dried under nitrogen and stored at 80°C prior to LC-MS. Targeted mass spectrometry (for PAHSA measurement) and untargeted lipidomic analysis (to determine relative fatty acid abundance) were performed as described previously (Yore et al., 2014; Zhang et al., 2016). Data from the untargeted lipidomics were analyzed with XCMS to identify changing metabolites between samples. Fatty acids were identified based on their mass/charge ratio and their abundance was normalized to tissue weight used for lipid extraction. Relative levels of each fatty acid species in AdChREBP KO samples were normalized to ChREBP$^{fl/fl}$ levels (Yore et al., 2014).

**Statistics**

All results are expressed as mean ± SEM. SigmaStat for Windows Version 3.5 was used to perform one-way ANOVA, or where indicated unpaired Student's t-test (for comparison of 2 groups) or two-way ANOVA with Holm Sidak post-hoc test (for comparison of 3 or more groups) to determine statistical validity of the data. A critical value of $p \leq 0.05$ was considered statistically significant.

**Supplementary References**

(2012). Polyethylene glycol [MAK Value Documentation, 1998]. The MAK Collection for Occupational Health and Safety. 248-270.
Aune, U.L., Ruiz, L., and Kajimura, S. (2013). Isolation and differentiation of stromal vascular cells to beige/brite cells. J Vis Exp.
Bligh, E.G., and Dyer, W.J. (1959). A rapid method of total lipid extraction and purification. Can J Biochem Physiol *37*, 911-917.
Blot, V., and McGraw, T.E. (2008). Use of quantitative immunofluorescence microscopy to study intracellular trafficking: studies of the GLUT4 glucose transporter. Methods Mol Biol *457*, 347-366.
Bruss, M.D., Khambatta, C.F., Ruby, M.A., Aggarwal, I., and Hellerstein, M.K. (2010). Calorie restriction increases fatty acid synthesis and whole body fat oxidation rates. Am J Physiol Endocrinol Metab *298*, E108-116.
Carvalho, E., Schellhorn, S.E., Zabolotny, J.M., Martin, S., Tozzo, E., Peroni, O.D., Houseknecht, K.L., Mundt, A., James, D.E., and Kahn, B.B. (2004). GLUT4 overexpression or deficiency in adipocytes of transgenic mice alters the composition of GLUT4 vesicles and the subcellular localization of GLUT4 and insulin-responsive aminopeptidase. J Biol Chem *279*, 21598-21605.
Eguchi, J., Wang, X., Yu, S., Kershaw, E.E., Chiu, P.C., Dushay, J., Estall, J.L., Klein, U., Maratos-Flier, E., and Rosen, E.D. (2011). Transcriptional control of adipose lipid handling by IRF4. Cell Metab *13*, 249-259.
Ellacott, K.L., Morton, G.J., Woods, S.C., Tso, P., and Schwartz, M.W. (2010). Assessment of feeding behavior in laboratory mice. Cell Metab *12*, 10-17.
Engelking, L.J., Kuriyama, H., Hammer, R.E., Horton, J.D., Brown, M.S., Goldstein, J.L., and Liang, G. (2004). Overexpression of Insig-1 in the livers of transgenic mice inhibits SREBP processing and reduces insulin-stimulated lipogenesis. J Clin Invest *113*, 1168-1175.
Herman, M.A., Peroni, O.D., Villoria, J., Schon, M.R., Abumrad, N.A., Bluher, M., Klein, S., and Kahn, B.B. (2012). A novel ChREBP isoform in adipose tissue regulates systemic glucose metabolism. Nature *484*, 333-338.
Jurczak,M.J., Lee, A.H., Jornayvaz, F.R., Lee, H.Y., Birkenfeld, A.L., Guigni, B.A., Kahn, M., Samuel, V.T., Glimcher, L.H., Shulman, G.I. (2012). Dissociation of inositol-requiring enzyme (IRE1α)-mediated c-Jun N-terminal kinase activation from hepatic insulin resistance in conditional X-box-binding protein-1 (XBP1) knock-out mice. J Biol Chem 287, 2558–2567.Karylowski, O., Zeigerer, A., Cohen, A., and McGraw, T.E. (2004). GLUT4 is retained by an intracellular cycle of vesicle formation and fusion with endosomes. Mol Biol Cell *15*, 870-882.
Moraes-Vieira, P.M., Yore, M.M., Dwyer, P.M., Syed, I., Aryal, P., and Kahn, B.B. (2014). RBP4 activates antigen-presenting cells, leading to adipose tissue inflammation and systemic insulin resistance. Cell Metab *19*, 512-526.
Perry, R.J., Camporez, J.P., Kursawe, R., Titchenell, P.M., Zhang, D., Perry, C.J., Jurczak, M.J., Abudukadier, A., Han, M.S., Zhang, X.M., *et al.* (2015). Hepatic acetyl CoA links adipose tissue inflammation to hepatic insulin resistance and type 2 diabetes. Cell *160*, 745-758.
Vazirani, R.P., Verma, A., Sadacca, L.A., Buckman, M.S., Picatoste, B., Beg, M., Torsitano, C., Bruno, J.H., Patel, R.T., Simonyte, K., *et al.* (2016). Disruption of Adipose Rab10-Dependent Insulin Signaling Causes Hepatic Insulin Resistance. Diabetes *65*, 1577-1589.

Yore, M.M., Syed, I., Moraes-Vieira, P.M., Zhang, T., Herman, M.A., Homan, E.A., Patel, R.T., Lee, J., Chen, S., Peroni, O.D., *et al.* (2014). Discovery of a class of endogenous mammalian lipids with anti-diabetic and anti-inflammatory effects. Cell *159*, 318-332.
Zhang, T., Chen, S., Syed, I., Stahlman, M., Kolar, M.J., Homan, E.A., Chu, Q., Smith, U., Boren, J., Kahn, B.B., *et al.* (2016). A LC-MS-based workflow for measurement of branched fatty acid esters of hydroxy fatty acids. Nat Protoc *11*, 747-763.